



Fermi National Accelerator Laboratory

FERMILAB-Conf-89/89

**Coherent Betatron Instability
Driven by Electrostatic Separators -
Stability Analysis of the TEVATRON***

F. A. Harfoush and S. A. Bogacz
Fermi National Accelerator Laboratory
P.O. Box 500, Batavia, Illinois 60510

March 1989

* Presented at the 1989 IEEE Particle Accelerator Conference, Chicago, Illinois, March 20-23, 1989.



COHERENT BETATRON INSTABILITY DRIVEN BY ELECTROSTATIC
SEPARATORS – STABILITY ANALYSIS OF THE TEVATRON

F.A. Harfoush and S.A. Bogacz
Accelerator Theory Department, Fermi National Accelerator Laboratory* ,
P.O. Box 500, Batavia, IL 60510

This paper outlines possible intensity limits due to the coherent betatron motion for the upgraded Tevatron with the electrostatic separators. Numerical simulation shows that this new vacuum chamber structure dominates the high frequency part of the coupling impedance spectrum and more likely will excite a slow head-tail instability. A simple stability analysis yields the characteristic growth-time of the unstable modes.

Coherent Betatron Motion

As was shown in Ref.1, through a systematic numerical analysis of Sacherer's model², the resulting growth-time vs chromaticity plots suggest existence of the $l \geq 1$ slow head-tail modes as a plausible mechanism for the observed coherent betatron instability. This last claim is based on a very good agreement between the measured values of the instability growth-time and the ones calculated on the basis of presented model.¹

One obviously expects, that even more pronounced version of this instability will also be present in the proposed high-intensity upgrades. Therefore, we should examine its prospective strength in the Tevatron with the new electrostatic separators. Encouraged by the successful explanation of the Tevatron's instability¹ we will apply the same intuitive model of the slow head-tail instability to examine the impact of the separators on this instability.

Following Sacherer's model² one assumes that the amplitude of the transverse beam oscillation (related to the pick-up monitor signal) is a superposition of a standing plane wave pattern (with the number of internal nodes defining the longitudinal mode index l) and a propagating part describing the betatron phase lag/gain, governed by the characteristic chromatic frequency, $\omega_\xi = \xi\omega_\sigma/\eta$. One can easily find the power spectrum of the transverse beam signal by taking the Fourier transform of the amplitude signal. The resulting beam spectrum is shifted by ω_ξ due to the presence of the propagating wave component (finite chromaticity). Periodicity given by the revolution period, $2\pi/\omega_0$, yields the discrete frequency spectrum with spacing ω_0 .

$$\omega_p = (p + \nu)\omega_0, \quad (1)$$

where p is an integer. The explicit form of the power spectrum is given by the following expression²

$$\rho^l(\omega) = \frac{h^l(\omega)}{\sum_{p=-\infty}^{\infty} h^l(\omega_p)}, \quad (2)$$

where

$$h^l(\omega) = \frac{4}{\pi^2} (l+1)^2 \frac{1 + (-1)^l \cos(2\omega\hat{\tau})}{[(2\omega\hat{\tau}/\pi)^2 - (l+1)^2]}.$$

Here $\hat{\tau}$ is the rms bunch-length in sec and h^l will serve as a spectral density function in evaluation of the averaged transverse coupling impedance.

Following Sacherer's argument³, one can generalize a simple equation of motion describing a wake field driven coherent betatron motion of a coasting beam to model the head-tail instability of the bunched beam. A simple dipole oscillation of the individual Fourier components of the beam is governed by the following equation³

$$(\nu\omega_0)^2 - \Omega_l^2 - i \frac{e\beta I_0}{\gamma m_0 2\hat{c}} \frac{1}{(l+1)^2} \sum_{p'=-\infty}^{\infty} Z_{\perp}(\omega_{p'}) \rho^l(\omega_{p'} - \omega_\xi) = 0. \quad (3)$$

The imaginary part of the coherent frequency, Ω_l , (with the negative sign) represents the inverse growth-time and is expressed by the following formula

$$\frac{1}{\tau^l} = - \frac{ce\beta I_0}{4\pi E\nu} \text{Re } Z_{\text{eff}}^l, \quad (4)$$

where E , is the total energy of a proton and the effective impedance is defined as follows

$$Z_{\text{eff}}^l = \frac{2\pi}{(l+1)^2} \frac{1}{2\omega_0\hat{\tau}} \sum_{p'=-\infty}^{\infty} Z_{\perp}(\omega_{p'}) \rho^l(\omega_{p'} - \omega_\xi) \quad (5)$$

The above result can be compared with the growth-time obtained in the framework of the Vlasov equation-based description of the slow head-tail instability. The so-called "air bag" model³ has exactly the same generic form as given by Eq.(4) with the effective impedance introduced as an average over a different set of spectral density functions; namely the Bessel functions of the first kind.

In order to evaluate the effective impedance, given by Eq.(5), one has to convolute the transverse impedance, which will be discussed in the next section, with the beam spectrum, Eq.(2). The result of the above summation obviously depends on chromaticity.

Transverse Coupling Impedance

Our consideration will be confined to the real part of the impedance only, since the imaginary part does not enter explicitly into the growth-time formulae given by Eqs.(4) and (5). We tentatively identified five dominant sources of the transverse impedance: electrostatic separators, kicker magnets, bellows, beam position monitors, resistive wall and magnet laminations.

Here we will concentrate on the first contribution induced by a set of 24 electrostatic separators, since the remaining four contributions have already been discussed⁴. Geometry of a single unit is depicted in Fig.1. The transverse coupling impedance was evaluated numerically using the MAFIA code (real time solution of the Maxwell equations for a given geometry excited by a Gaussian test bunch). Calculated Fourier transform of the transverse wake field is translated into the transverse impedance in Ohm/m. The resulting solution is illustrated in Figs. 2 and 3.

The above contribution will serve as a starting point for calculation of the effective impedance, which will be carried out in the next section.

* Operated by the Universities Research Association, Inc. under contract with the U.S. Department of Energy

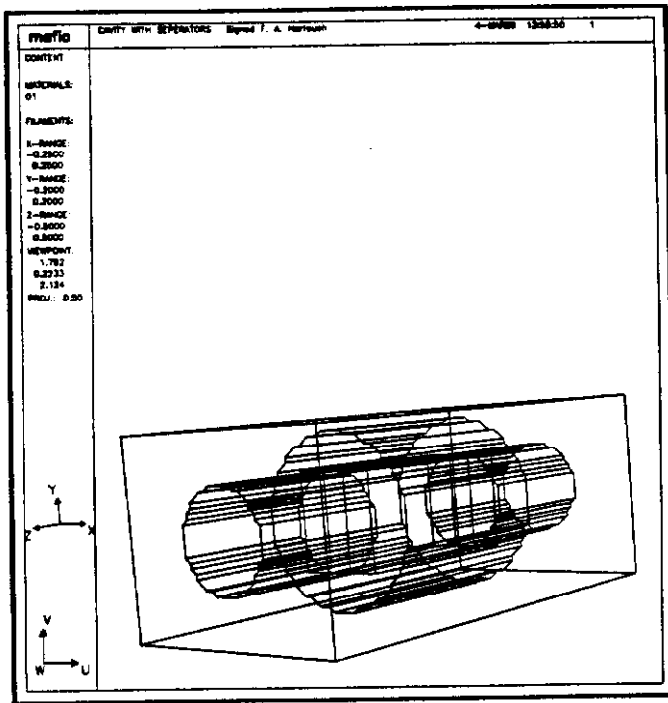


Fig.1

Effective Impedance

In order to evaluate the effective impedance one has to convolute the transverse impedance with the beam spectrum according to Eq.(5). The result of the above summation obviously depends on chromaticity.

One can notice (see Figs.2 and 3) that the transverse impedance $Z_{\perp}(\omega)$ has a diffraction-like character; a principle maximum of width $\lambda = \pi c/L$ at the origin and a series of equally spaced secondary maxima governed by the same width. Similarly,

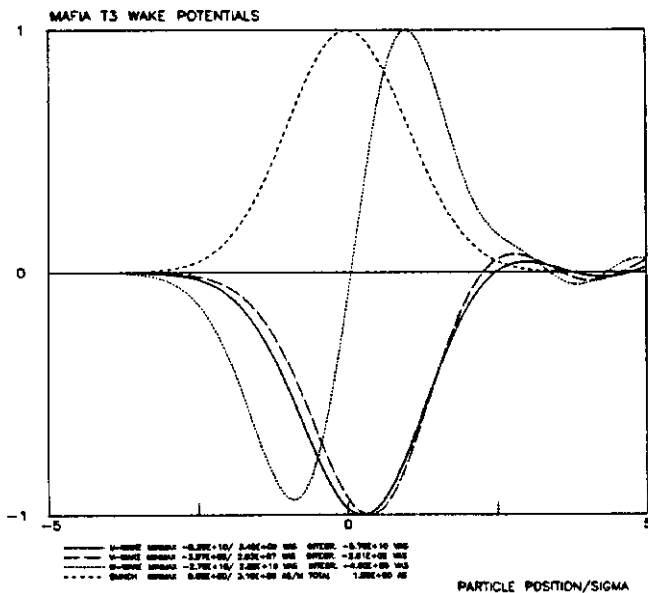


Fig.2

Transverse Impedance for a Cavity with Separators

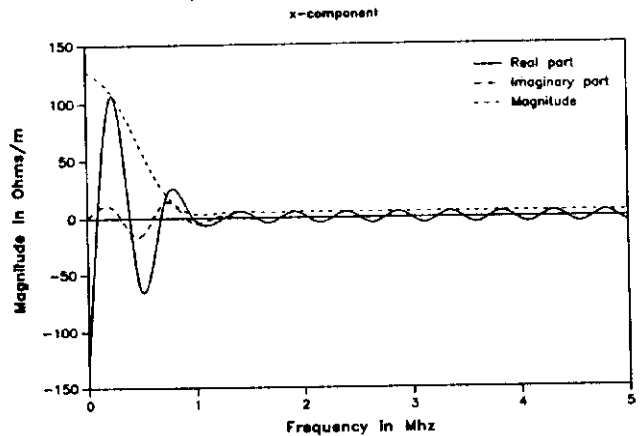


Fig.3

the harmonics of the beam spectrum, $\rho(\omega - \omega_k)$, have one ($l=0$) or a

pair ($l \geq 1$) of principle maxima of width $\epsilon = \pi / 2\hat{\alpha}$ followed by a sequence of secondary maxima. Both spectra are sampled by a discrete set of frequencies, $\omega_p = (p + \nu)\omega_0$. In case of relatively long proton bunches in the Tevatron, both widths λ and ϵ are comparable and they are of the order of the chromatic frequency, ω_k , evaluated at about 10 units of chromaticity. These features combined with the convolution formula for the effective impedance, Eq.(5), result in substantial 'overlap' of the transverse impedance and the beam spectrum, which in turn leads to large values of effective impedance for relatively small chromaticities ($\xi \sim 10$).

Growth-Time Summary

Assuming only one dominant contribution to the transverse coupling impedance (due to the electrostatic separators), the inverse growth-times were calculated numerically according to Eqs.(1)-(5). The study was done at the injection energy (150 GeV), since the instability growth-rate is inversely proportional to energy. For the purpose of this model calculation we assumed a train of high intensity (3×10^{11} ppb), relatively long ($\epsilon = 2.5$ eV-sec), proton bunches injected into the Tevatron. The transverse beam size is given by the normalized rms emittance of $\epsilon = 4 \pi$ mm mrad. The resulting growth-rates as a function of chromaticity evaluated for different slow head-tail modes ($l = 0, 1, 2, 3$) are illustrated in Fig.4. Furthermore, the results are summarized in Table 1. One can immediately see a qualitative difference between the $l=0$ and $l \geq 1$ modes; the $l=0$ mode is always stable for positive chromaticities, while the stability of the $l \geq 1$ modes strongly depends on chromaticity and longitudinal emittance of the bunch. Table 1 collects extreme values of the characteristic growth-times, τ_l^c , for various slow head-tail modes, l , together with the values of chromaticity, ξ_{max} , corresponding to the most unstable points of the above modes. The Tevatron is dominated by the $l=2$ mode of the slow head-tail instability. One can see (Table 1) that the lowest mode is stable ($l=0$) and the most unstable mode ($l=2$) is characterized by the growth-time $\tau^l = 10 \times 10^{-3}$ sec.

ϵ [eV-sec.]	ν_{β}	l	ξ_{\max}	τ^l [sec]
Tevatron (p-injection) @ 150 GeV, $N = 3 \times 10^{11}$ ppb				
2.5	19.456	0	stable mode	
		1	3	33×10^{-3}
		2	5	10×10^{-3}
		3	25	13×10^{-3}

Table 1

Tevatron (p-injection @ 150 GeV) $N = 3.E11$ ppb
 $\epsilon = 2.5$ eV-sec

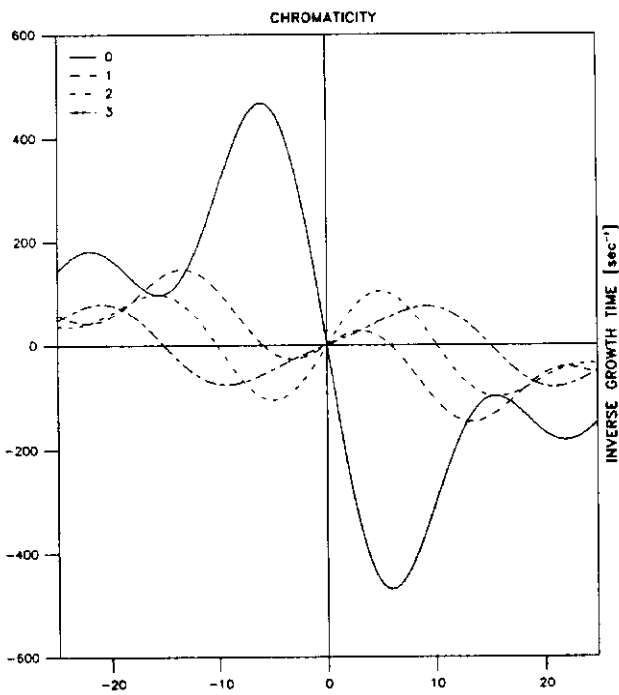


Fig.4

References

- [1] S.A. Bogacz, M. Harrison and K.Y. Ng, FERMILAB FN-485, (1988)
- [2] F. Sacherer, Proc. 9-th Int. Conf. on High Energy Accelerators, Stanford 1974, p. 347
- [3] F. Sacherer, CERN/SI-BR/72-5 (1972), unpublished
- [4] S.A. Bogacz, FERMILAB FN-498, (1988)